COMMUNICATION

Solvent-Annealed Crystalline Squaraine: $PC_{70}BM$ (1:6) Solar Cells

*Guodan Wei, Siyi Wang, Kai Sun, Mark E. Thompson, and Stephen R. Forrest**

Efficient bulk heterojunction (BHJ) solar cells are characterized by a large interface area between donor and acceptor materials that ensures efficient photogenerated exciton dissociation into free charge. The optimal scale of the phase separation between these consistuents is that of the exciton diffusion length (L_D), and the separated phases must be contiguous to allow for low-resistance charge transport pathways from the photosensitive region to the electrodes.[1–6] To realize such a BHJ nanostructure, techniques such as thermal[7] and solvent-vapor annealing[8] have been demonstrated. The most successful processing protocols affect the aggregation and morphology in a predictable and and controlled manner. In past work, we have shown that solution-processed squaraine (SQ), followed by vacuum thermally evaporated C_{60} donor/acceptor solar cells can have power conversion efficiencies of $\eta_p = 4.6 \pm 0.1\%$ when they are fabricated into a lamellar device that is subsequently annealed at high temperature (110 °C).[9] It was found that the annealing roughens the SQ surface, thereby creating a highly folded BHJ interface with the C_{60} and thus compensating for the very short (1.6 ± 0.2 nm) L_D characteristic of the SQ donor. Although the L_D of SQ is very small, this deficiency is partially compensated by its high absorption coefficient compared to that of C_{60}. This motivates the use of SQ:fullerene blends, whereby the ratio of materials strongly favors that of the fullerene to take advantage of its large L_D and low absorption. In previous work this approach has been partially successful, with the highest external quantum efficiencies (*EQE*) under low intensity illumination of SQ:$PC_{70}BM$ (1:6) blends approaching 50% across the visible spectrum. Unfortunately, devices fabricated using such blends exhibited exceptionally low fill factors (*FF*~0.35) due to a large internal series resistance to charge extraction from the low density of SQ in the mixture. Hence, under standard simulated solar illumination conditions (100 mW/cm^2, AM1.5G spectrum), the efficiency was limited to only ~3%.[10]

G. Wei, Dr. K. Sun, Prof. S. R. Forrest
Department of Materials Science and Engineering
University of Michigan
Ann Arbor, MI 48109, USA
E-mail: stevefor@umich.edu
S. Wang, Prof. M. E. Thompson
Department of Chemistry
University of Southern California
Los Angeles, CA 90089, USA
Prof. S. R. Forrest
Departments of Electrical Engineering
and Computer Science, and Physics
University of Michigan
Ann Arbor, MI 48109, USA

DOI: 10.1002/aenm.201100045

In this work, we explore annealing of these SQ:$PC_{70}BM$ (1:6) blends in solvent vapor to create continuous crystalline (and hence low resistance) pathways for hole conduction through the rareified SQ environment. We note that, while spin-casting of these mixtures provides a simple means to prepare homogeneous thin films, rapid solvent evaporation does not allow for sufficient molecular reorganization, which is needed to achieve an equilibrium, crystalline, and uniformly phase-separated mixture.[11–14] We find that post-annealing through additional extended exposure of the blend to dichloromethane (DCM) can lead to a more optimized morphology that reduces series resistance, and hence increases the *FF* to 0.50 ± 0.01 and a power conversion efficiency of $\eta_p = 5.2 \pm 0.3\%$ of the resulting cells under AM1.5G, 1 sun simulated solar emission (corrected for spectral mismatch). Indeed, our best cells measured reached efficiencies of 5.5% under similar standard conditions.

Post-annealing of SQ:$PC_{70}BM$ (1:6) blends entails the 6 min to 30 min exposure of the films to DCM vapors in a closed glass vial enclosed in an ultra-high-purity nitrogen-filled glove-box at room temperature (see Experimental Section). As shown in **Figure 1**, the lack of an X-ray diffraction (XRD) peak for as-deposited SQ:$PC_{70}BM$ films indicates an amorphous structure. In contrast, after annealing for 10 min, a peak appears at $2\theta = 7.80 \pm 0.08^0$ that increases in intensity when the annealing time is extended to 30 min. This peak is the (001) reflection of SQ, corresponding to an intermolecular spacing of 11.26 ± 0.16 Å. After a 30 min exposure to DCM, a second peak corresponding to the (002) reflection appears, indicating a continued increase in order.[9] The mean crystal sizes of SQ in the blends annealed for 12 min and 30 min are estimated to be 2.0 ± 0.2 nm and 51 ± 4 nm, respectively, inferred from the XRD peak broadening using the Scherrer method.[15]

The root-mean-square roughness obtained from the atomic force microscopy (AFM) images (**Figure 2**a) of the as-cast film is 0.8 ± 0.1 nm. In contrast, the roughness of the blend after 12 min solvent annealing increases to 8.4 ± 1.2 nm (Figure 2b), indicating substantial roughening due to the polycrystalline growth of SQ in the mixture. With even longer annealing of 30 min, the phase separation of SQ and $PC_{70}BM$ continues, as indicated by further roughening to 12.0 ± 1.4 nm (Figure 2c). The roughening, which is in part due to phase separation, has also been observed in transmission electron microscopy (TEM) imaging (Figure 2c) and surface phase images measured by AFM (the inset in Fig. 2c). The average crystal domain size also increases concomitant with the roughening, as noted above from the XRD line broadening.

The spectra in the visible range for the as-cast and four DCM solvent-annealed SQ:$PC_{70}BM$ blended films on quartz substrates are shown in **Figure 3**a. The absorption coefficient of SQ throughout the entire observed spectral range increases with

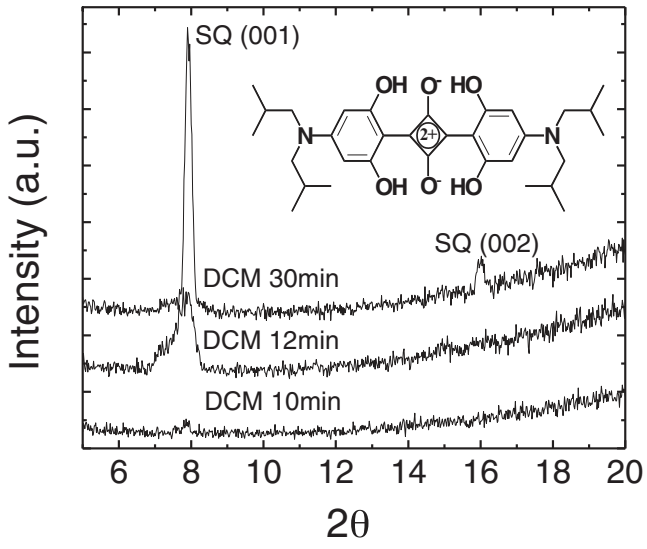

Figure 1. The X-ray diffraction patterns for squaraine (SQ) :$PC_{70}BM$ (1:6) films annealed in dichloromethane (DCM) solvent for 10min, 12 min, and 30 min. The inset shows the molecular structure of SQ.

annealing time of up to 8 min, but as time is further increased, the change becomes saturated. Note also, that the crystalline blend film (DCM 12 min) has a less pronounced absorption peak at $\lambda = 680$ nm than in the amorphous films.

The photoluminescence (PL) intensity of a film is quenched in the presence of charge transfer from photogenerated donor excitons to acceptor molecules. Therefore, efficient PL quenching in the SQ:$PC_{70}BM$ blends indicates efficient exciton dissociation due to photogeneration within a distance, L_D, of an interface.[16–17] As above, the relevant length scales are 1.6 nm for SQ, and 20 nm to 40 nm for $PC_{70}BM$. In our experiments, a 10 min anneal results in a maximum PL intensity quenching, followed by a reduction in quenching as the annealing time is further increased. This is understood in terms of our values of L_D and mean crystallite size, δ. The PL quenching is strongest when $L_D \sim \delta \sim 2$ nm after approximately 10–12 min annealing. Additional annealing leads to initiation of further phase segregation of the crystals, at which point $\delta >> L_D$, and hence the excitons are no longer efficiently transported to a dissociating heterointerface.[18]

The *EQE* of the as-cast and solvent-annealed solar cells in Figure 3c indicate a similarly broad spectral response to the absorption, extending from a wavelength of $\lambda = 300$ nm to $\lambda = 750$ nm. The *EQE* peak of SQ increases from 26 ± 2% (as-cast) to 60 ± 1% (annealed for 10 min). After a 12 min anneal, the peak *EQE* is reduced to < 40% across the entire wavelength range. These results, directly analogous to those obtained in absorption, further indicate that the cell efficiency depends strongly on crystallite size, with the optimum size comparable to L_D, thereby leading to maximum exciton diffusion to the dissociating donor/acceptor interface between SQ and $PC_{70}BM$.

The *J-V* characteristics in Figure 3d measured under 1 sun, AM1.5G simulated solar emission, indicate that the short-circuit current density (J_{sc}) is substantially enhanced from 6.9 mA/cm^2 (as-cast) to 12.0 mA/cm^2 (10 min solvent anneal), and then

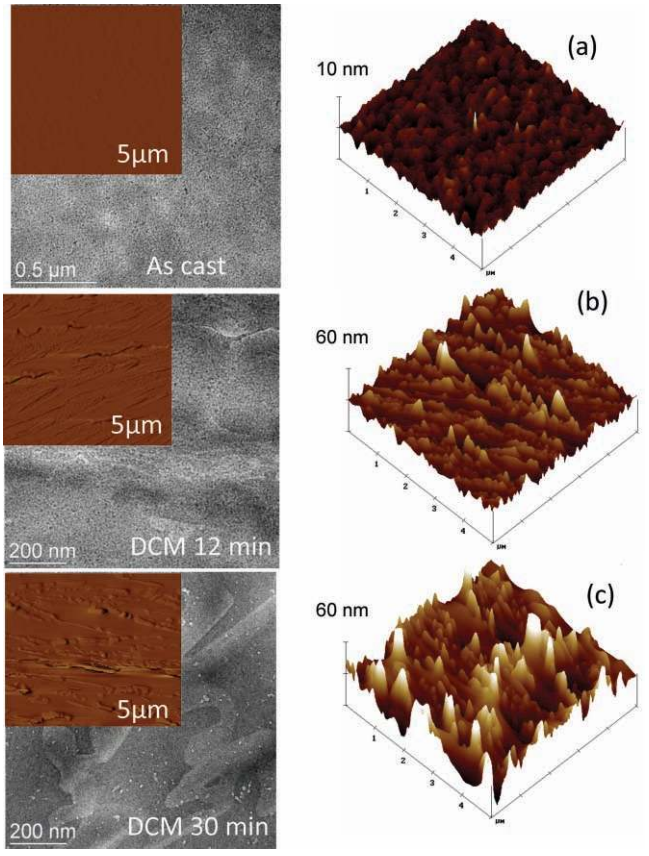

Figure 2. The effects of dichloromethane (DCM) solvent on film morphology. Transmission electron microscopy and AFM images of squaraine (SQ):$PC_{70}BM$ (1:6) films: a) as-cast, b) annealed in DCM for 12 min, and c) annealed in DCM for 30 min. The inset shows the surface images measured by AFM.

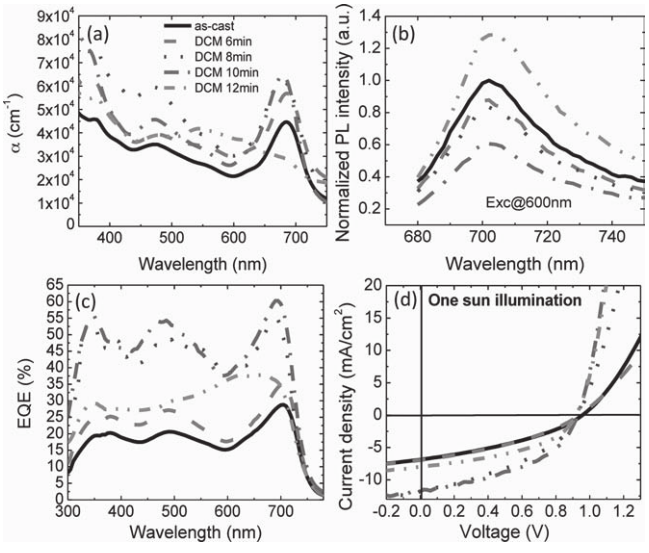

Figure 3. The effect of dichloromethane (DCM) solvent annealing as a function of time on squaraine:$PC_{70}BM$ composite films with respect to a) UV-vis absorption spectra, b) photoluminescence (PL), c) external quantum efficiencies (*EQE*), and d) the current density vs. voltage (*J–V*) characteristics of the SQ:$PC_{70}BM$ (1:6) cells at 1 sun illumination.

decreases to 8.3 mA/cm^2 after 12 min exposure to DCM. The *FF* shows a similar dependence on annealing time, indicating that the extended order decreases the series resistance, as anticipated for crystalline organic materials with improved molecular packing. Fitting the forward *J–V* curves using the modified diode equation[10] yields the specific series resistance, R_{SA}. The as-cast cell has $R_{SA} = 35.2 \pm 1.0\ \Omega \cdot cm^2$, then gradually reduces to $5.0 \pm 0.5\ \Omega \cdot cm^2$ when the annealing time is 12 min. However, further increase of DCM annealing time increases the density of pinholes between active layer and the contacts, leading to shorted diodes.

The optical and electrical changes on annealing lead directly to an increase in η_p, as shown in **Figure 4**a. Here, the as-cast cell η_p increases slightly with power intensity, then levels offto 2.4 ± 0.1% at 1 sun, along with a concomitant decrease in *FF* from 0.40 ± 0.02 (at 0.002 sun) to 0.36 ±0.01 (1 sun) (see Figure 4b). In contrast, for the 10 min annealed cell, the *FF* increases from 0.42 ± 0.01 (0.002 sun) to 0.50 ± 0.01 (1 sun), while η_p correspondingly increases from 1.5 ± 0.1% to 5.2 ± 0.3% (1 sun), with a peak measured value for a cell in this population of 5.5% (J_{SC} = 12.0 mA/cm^2, *FF* = 0.5 and open-circuit voltage (V_{oc}) = 0.92 V). Finally, the 12 min annealed cell shows a roll off in η_p of 3.2 ± 0.1%, due to the reduced *EQE* and *FF*. We note that squaraine molecules with dicyanovinyl groups have been reported[22] that extend the photon absorption to 900 nm, and exhibit J_{sc} = 12.6 mA/cm^2 although the V_{oc} is considerably lower, leading to η_p<2%.

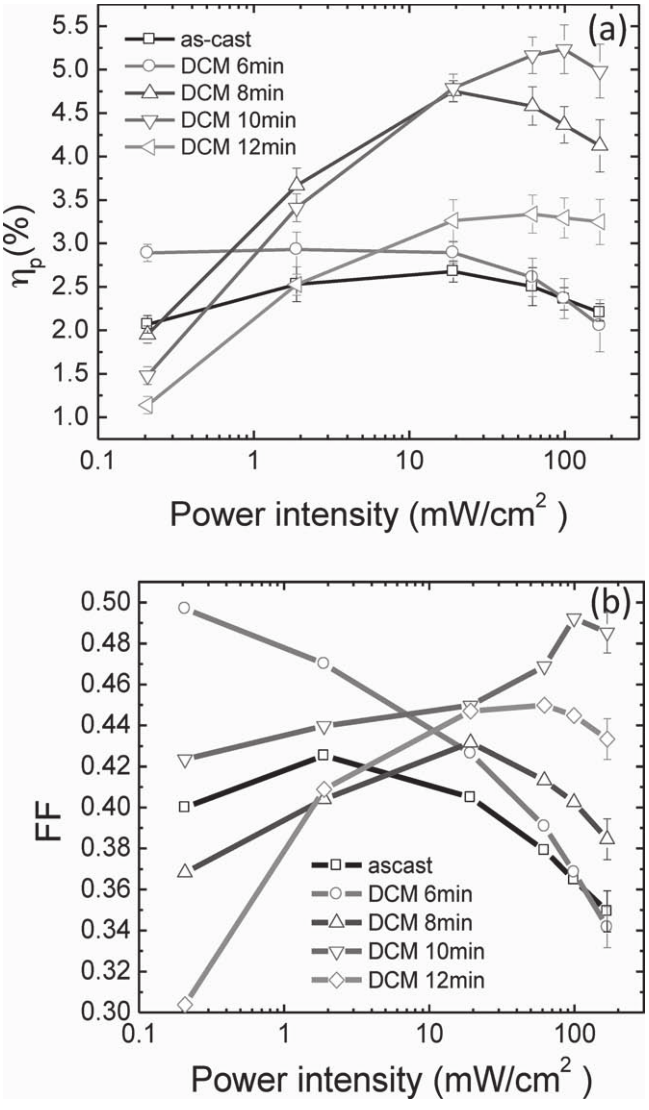

Figure 4. a) The power conversion efficiency (η_p) and b) fill factor (*FF*) versus power intensity as a function of dichloromethane (DCM) solvent annealing time, for the device structure of ITO/MoO_3(80 Å)/SQ:$PC_{70}BM$ (1:6 780 Å)/C_{60}(40 Å)/BCP(10 Å)/LiF(8 Å)/Al(1000 Å).

In conclusion, DCM solvent annealing leads to control of the nanoscale phase separation of SQ:$PC_{70}BM$ (1:6) organic films. Through optimizing morphology and molecular ordering of the SQ:$PC_{70}BM$ (1:6) solar cells, a peak power conversion efficiency of 5.5 ± 0.3% has been achieved in these blended structures, with a maximum cell performance achieved when the exciton diffusion length is approximately equal to the mean SQ crystallite size. This precise structural control takes advantage of the high absorption coefficient yet small diffusion length characteristic of this squaraine compound, allowing for only very dilute SQ;$PC_{70}BM$ mixtures to result in high solar cell efficiency.

Experimental Section

X-ray-diffraction (XRD) patterns of the SQ:$PC_{70}BM$ (in relative weight concentrations of 1:6) thin films spin-coated 1000 rpm for 30 s on indium tin oxide (ITO)-coated glass substrates precoated with 80 Å MoO_3 at a low rate of 1000 rpm (revolutions per minute) were obtained using a Rigaku diffractometer in the θ-2θ geometry using a 40 kV Cu K_α radiation source. The thicknesses of the SQ:$PC_{70}BM$ (1:6) blend cast from 42 mg/mL solutions in 1,2 dichlorobenzene (DCB) heated on a hotplate for 12 h, as determined by using Woolam VASE ellipsometer, were 780 Å.

Atomic force microscopy (AFM) images were collected in a Nanoscope III AFM in the tapping mode. Solvent annealing of SQ:$PC_{70}BM$ (1:6) deposited films was done in a closed glass vial filled with 1 mL dichloromethane (DCM) for a time varying from 6 min to 30 min. For transmission electron microscopy (TEM) studies, the SQ:$PC_{70}BM$ (1:6) films on ITO substrate coated with 80 Å MoO_3 were immersed in deionized (DI) water for 1 h. Next, the MoO_3 was dissolved in water, and the organic layers were floated on the surface of the DI water. Then the as-cast and solvent annealed SQ:$PC_{70}BM$ (1:6) films were transferred onto amorphous carbon film coated Cu grids. The TEM images were taken using a 200 kV JEOL 2010F analytical electron microscope.

The absorption spectra of the as-cast and four DCM annealed films on quartz substrates were measured using a Perkin-Elmer Lambda 1500 UV-NIR spectrometer. Photoluminescence (PL) was measured at an excitation wavelength of λ = 600nm.[9] Solar cell structures employed the following structure: ITO/MoO_3 (80 Å)/SQ:$PC_{70}BM$ (1:6 780 Å)/C_{60} (40 Å)/BCP (10 Å)/Al (1000 Å) (BCP: bathocuproine). Here, MoO_3 is thermally evaporated onto the ITO surface in a vacuum system with a base pressure of 10^{-7} torr. Following spin-casting deposition and solvent annealing, devices were completed by thermally evaporating a 8 Å thick LiF and 1000 Å thick Al cathode through a shadow mask, resulting in a device area of 8×10^{-3} cm^2. The current density-voltage (*J–V*) characteristics and power conversion efficiency (η_p) of the devices were measured using an Oriel 150 W solar simulator irradiation from a Xe arc lamp with AM1.5G filters and an National Renewable Energy Laboratory (NREL)-calibrated standard Si detector. Measurements and solar spectral correction were made using standard methods.[22] The *EQE* was measured using monochromatic light from a Xe-lamp was chopped at 200 Hz and focused to the device active area.

Acknowledgements

This work was supported in part by the Air Force Office of Scientific Research (GW), Energy Frontier Research Centers: The Center for Solar and Thermal Energy Conversion at the University of Michigan (Award No. DE-SC00000957, SRF), the Department of Energy Energy Frontier Center at the University of Southern California (award DE-SC0001011, MET), and Global Photonic Energy Corp. (SW). We also thank for Richard R. Lunt, Yifan Zhang and Jeramy D. Zimmerman for helpful discussions and technical assistance.

Received: November 17, 2010
Revised: January 11, 2011
Published online: February 9, 2011

[1] P. Peumans , S. Uchida , S. R. Forrest, *Nature* **2003**, *425*, 158.
[2] H. Hoppe, N. S. Sariciftci, *J. Mater. Chem.* **2006**, *16*, 45.
[3] B. Walker, A. B. Tamayo, X. D. Dang, P. Zalar, J. H. Seo, A. Garcia, M. Tantiwiwat, T. Q. Nguyen, *Adv. Funct. Mater.* **2009**, *19*, 3063.
[4] C. V. Hoven, X. D. Dang, R. C. Coffin, J. Peet, T. Q. Nguyen, G. C. Bazan, *Adv. Mater.* **2010**, *22*, 63.
[5] M. C. Scharber, D. Wuhlbacker, M. Koppe, P. Denk, C. Waldauf, A. J. Heeger, C. L. Brabec, *Adv. Mater.* **2006**, *18*, 789.
[6] M. Campoy-Quilers, T. Ferenczi, T. Agostinelli, P. G. Etchegoin, Y. Kim, T. D. Anthopoulos, P. N. Stavrinou, D. D. C. Bradley, J. Nelson, *Nat. Mater.* **2008**, *7*, 158.
[7] W. L. Ma, C. Y. Yang, X. Gong, K. Lee, A. J. Heeger, *Adv. Funct. Mater.* **2005**, *15*, 1617.
[8] G. D. Sharma, P. Suresh, S. S. Sharma, Y. K. Vijay, J. A. Mikroyannidis, *ACS Appl. Mater. Interfaces* **2010**, *2*, 504.
[9] G. D. Wei, R. R. Lunt, K. Sun, S. Y. Wang, M. E. Thompson, S. R. Forrest, *Nano Lett.* **2010**, *10*, 3555.
[10] G. D. Wei, S. Y. Wang, K. Renshaw, M. E. Thompson, S. R. Forrest, *ACS Nano* **2010**, *4*, 1927.
[11] Y. Yao, J. Hou, Z. Xu, G. Li, Y. Yang, *Adv. Funct. Mater.* **2008**, *18*, 1783.
[12] G. Li, V. Shrotriya, J. Huang, Y. Yao, Tommoriarty, K. Emery, Y. Yang, *Nat. Mater.* **2005**, *4*, 864.
[13] M. Morana, H. Azimi, G. Dennler, H. J. Egelhaaf, M. Scharber, K. Forberich, J. Hauch, R. Gaudiana, D. Waller, Z. Zhu, K. Hingerl, S. S. Bavel, J. Loos, C. J. Brabec, *Adv. Funct. Mater.* **2010**, *20*, 1180.
[14] F. Silvestri, M. D. Irwin, L. Beverina, A. Facchetti, G. A. Pagani, T. J. Marks, *J. Am. Chem. Soc.* **2008**, *130*, 17640.
[15] T. Erb, U. Zhokhavets, G. Gobsch, S. Raleva, B. Stühn, P. Schilinsky, C. Waldauf, C. J. Brabec, *Adv. Funct. Mater.* **2005**, *15*, 1193.
[16] T. M. Clarke, A. M. Ballantyne, S. Tierney, M. Heeney, W. Duffy, I. McCulloch, J. Nelson, J. R. Durrant, *J. Phys. Chem. C* **2010**, *114*, 8068.
[17] J. S. Kim, Y. Park, D. Y. Lee, J. H. Lee, J. H. Park, J. K. Kim, K. Cho, *Adv. Funct. Mater.* **2010**, *20*, 540.
[18] R. R. Lunt, J. B. Benziger, S. R. Forrest, *Adv. Mater.* **2010**, *22*, 1233.
[19] D. W. Sievers, V. Shrotriya, Y.Yang, *J. Appl. Phys.* **2005**, *100*, 114509.
[20] S. R. Forrest, *MRS Bull.* **2005**, *30*, 28.
[21] P. K. Watkins, A. B. Walker, G. L. B. Verschoor, *Nano Lett.* **2005**, *5*, 1814.
[22] V. Shrotriya, G. L., Y. Yao, T. Morarty, K. Emery, Y. Yang, *Adv. Funct. Mater.* **2006**, *16*, 2016.
[23] U. Mayerhoffer, K. Deing, K. Gruβ, H. Braunschweig, K. Meerholz, F. Würthner, *Angew. Chem. Int. Ed.* **2009**, *48*, 8776.